

Mineralisation predictive targeting using TensorFlow (Google) deep neural networks

Karl Kwan
Geotech Ltd.
Aurora, CAN
Karl.kwan@geotechairborne.com

Ian Johnson
Consultant
Toronto, CAN
ianjohnson@amtelecom.net

Jean M Legault*
Geotech Ltd.
Aurora, CAN
jean@geotech.ca

Kanita Khaled
Geotech Ltd.
Aurora, CAN
kanita.khaled@geotechairborne.

SUMMARY

Simple two-layer feedforward supervised neural network (NN) has been described and used for mineral predictive targeting. However, the simple NN has some limitations. For instance, it requires the geophysical responses of over the target be positively high relative to non-target areas.

The release of Google's TensorFlow (TF) for Python (<https://www.tensorflow.org/>) in 2015 has made it possible to apply the more powerful and robust Deep Neural Network (DNN) to geoscience data for mineral predictive targeting.

We test the TF DNN using the magnetic data over a kimberlite in the Canadian Shield and compare the results with those from the simple two-layer NN. The DNN results are better.

DNNs are applied to the helicopter TDEM data from Nuqrah, western Arabian Shield and the TDEM from Kabinakagami Lake greenstone belt in Superior craton in Ontario to illustrate the utility of predictive targeting of DNN..

Key words: Targeting,

INTRODUCTION

A neural network is an algorithm that can learn and apply what was learnt to new data. Neural networks, inspired by biological neurons, are composed of simple elements or neurons in parallel (Goodfellow et al., 2016). A neural network requires training, or supervised learning, with user specified inputs (geoscience-themed data or features) and outputs (targets or labels), in order to be useful.

In the case of mineral exploration using geophysical methods, the neural network learns by being given several grids representing different geophysical signatures of a target area and they are called the training grids (featured data). The training requires a target or label grid composed of 1's and 0's of the target area. The outputs consist of two classes of 1 and 0, 1 being the target usually a known ore deposit or mineralisation occurrence and 0 being non-target.

A simple neuron is illustrated in Figure 1. It consists of the scalar weight w , transfer function f . The input to the simple

neuron is the scalar p , and the output a , which is defined as $a=f(wp)$.

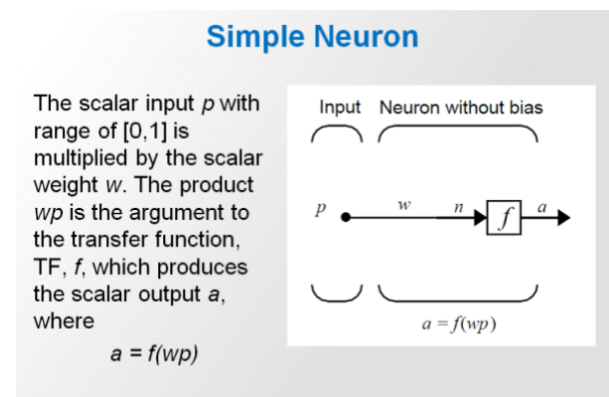


Figure 1. A simple neuron.

METHOD AND RESULTS

Deep Neural Networks

A Deep Neural Network (DNN) is a simple feedforward network with many hidden layers, as illustrated in Figure 2.

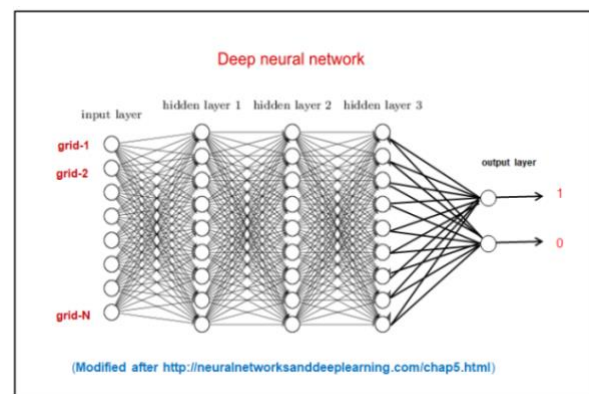


Figure 2. A simple three hidden layers DNN with two output classes, 1 and 0.

In general, it is believed that having more hidden layers can help DNN to make better predictions for large datasets and complex problems.

The useful outputs from DNN for predictive targeting are the target (1) probabilities, i.e., a grid cell with target probability of 1 meaning the ground covered by the grid cell could be a

target, and a grid cell with target probability of 0 meaning the ground covered by the grid cell should not be considered as a target.

Increasing the number of hidden layers may increase the DNN performance initially, but the performance reaches a plateau the number of hidden layers goes above ten or so, as empirically illustrated by Goodfellow et al. 2016 and provided in Figure 3.

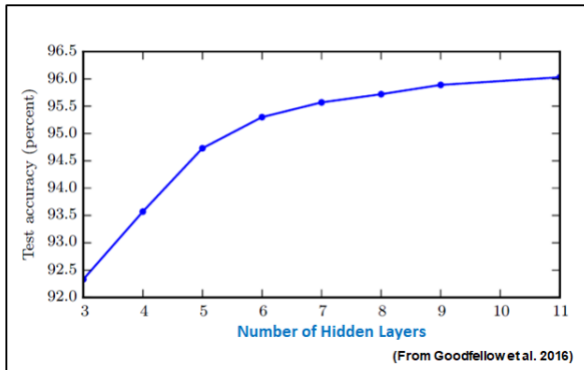


Figure 3. DNN prediction accuracy versus the number of hidden layers from empirical results of transcribing multi-digit numbers from photographs of addresses (Goodfellow et al., 2016).

A Simple Test of DNN

The release of Google’s TensorFlow (TF) for Python (<https://www.tensorflow.org/>) in 2015 has made it possible to apply the more powerful and robust Deep Neural Network (DNN) to geoscience data for mineral predictive targeting.

Helicopter time-domain electromagnetic (VTEM) test data were acquired over a known kimberlite in the Canadian Shield. The data are processed for AIP apparent chargeability, Cole-Cole time-constant TAU and the Tau-scaled chargeability (TSC) (Kwan et al., 2018). The Total Magnetic Intensity (TMI) and AIP data over the kimberlite are shown in Figure 4. The kimberlite was reversely magnetized during its emplacement.

The training area is a rectangle covering part of the kimberlite and the surrounds. The target is part of the kimberlite. The target definition grid is created, with 1’s in the target area and 0’s in non-target area.

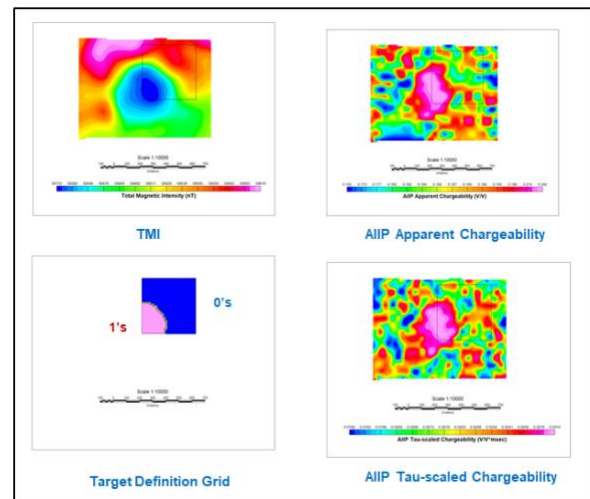


Figure 4. TMI, AIP apparent chargeability, AIP TSC test data, and target definition grids over a known kimberlite in the Canadian Shield.

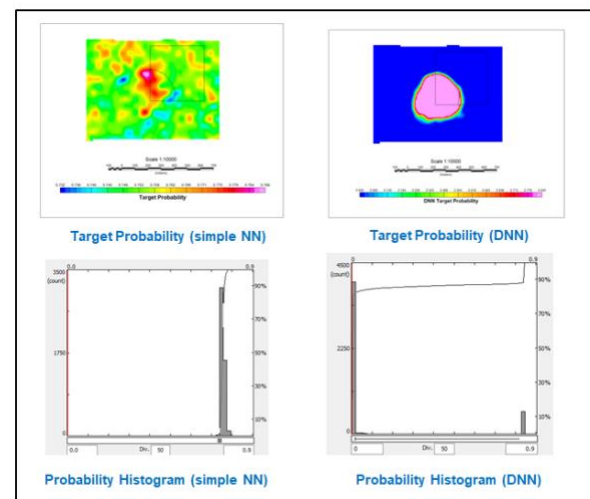


Figure 5. Target probabilities, gridded data and histogram, from simple NN (left) and DNN (right).

SEDEX Case Study

A case demonstrates the DNN predictive targeting for VMS mineralisation is conducted using TDEM data. In late 2011-early 2012, as part of a larger survey campaign in the western Arabian Shield, a helicopter VTEM (Versatile Time-domain ElectroMagnetic; Witherly et al., 2004) survey was flown over the 1.4 Mt Nuqrah sedimentary exhalative (SEDEX) copper–lead–zinc–gold massive sulphide deposits in order to determine their geophysical signatures (Legault et al., 2014).

The Nuqrah deposit comprises two mineralised bodies: Nuqrah North (0.4 Mt @ 0.75% Cu, 1.22% Pb, 6.0% Zn,) and the larger Nuqrah South (1.0 Mt @ 0.82% Cu, 1.83% Pb, 5.6% Zn) that are north-striking and 4 km apart, each marked by a gossan. At Nuqrah North the mineralisation is found in graphitic and chloritic tuff and dolomitic marble between andesite and rhyolitic tuff. The mineralised bodies are pod-like and parallel to bedding. At Nuqrah South, mineralisation is in the upper part of the dolomitic marble unit and in the lower part of a diabase intrusive, associated with graphitic rock and forming lenticular pods along the bedding.

Advanced interpretation products, i.e. EM induction time-constant TAU, Resistivity Depth Imaging (RDI) depth slices at 150 m and 300 m, AIP apparent chargeability and resistivity, are generated and are shown in Figure 6.

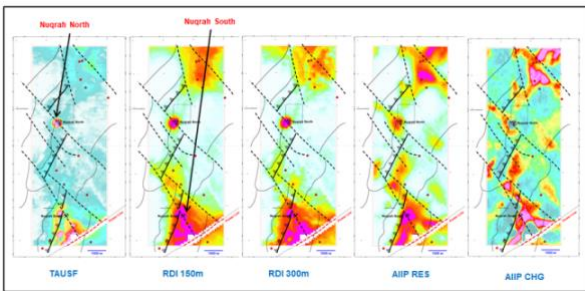


Figure 6. DNN test data from Nuqrah. Nuqrah North is located near the centre of the survey block and is used as the target for training.

An eight hidden-layers DNN is used for the VMS targeting of the Nuqrah test data. The DNN results of the top 70% target probability are shown in Figure 7. The DNN results identify the larger Nuqrah South deposit, as well as other targets, especially in the NE corner of the VTEM block.

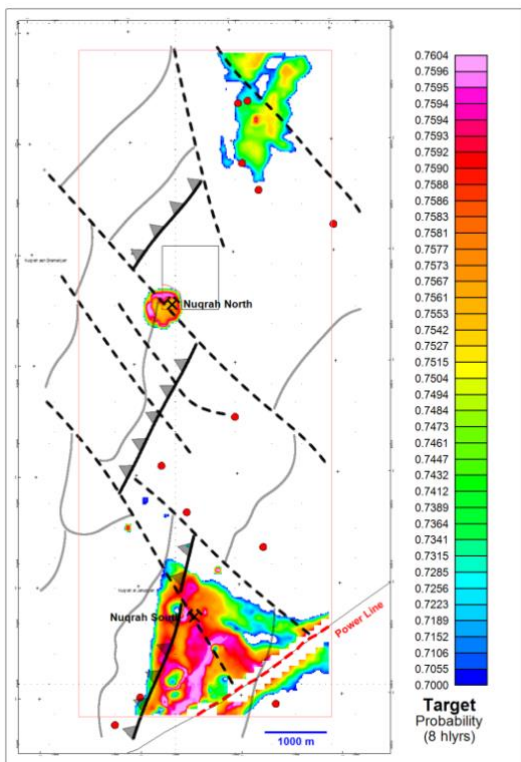


Figure 7. Top 70% target probabilities generated from a DNN with eight hidden layers; red dots indicate known SEDEX occurrences.

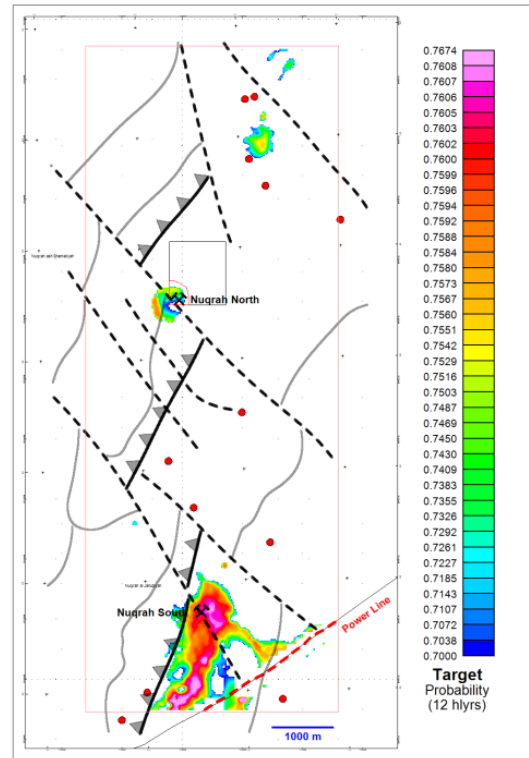


Figure 8. Top 90% target probabilities generated from a DNN with twelve hidden layers.

The results of using a DNN with twelve hidden layers are shown in Figure 8. The improvement over the results of eight hidden-layers DNN appears to be obtaining more focused targets.

Archean Greenstone-hosted Lode Gold Case Study

The direct detection of Archean greenstone-hosted lode disseminated gold mineralisation by geophysical methods is highly challenging and unfortunately rarely successful in exploration; detection is further complicated by the presence of minerals that have strong geophysical responses but are not of economic interest, for example, barren sulphides such as pyrrhotite (Mir et al., 2019). Notwithstanding the difficulty, we present an Archean greenstone-hosted lode gold case study.

During July and October 2014, Geotech Ltd carried out a helicopter VTEM survey over the Kabinakagami Lake Greenstone Belt (KLGB) on behalf of Ontario Geological Survey, Ministry of Northern Development and Mines (MNDM). The survey is located in northern Ontario south of Hearst, and acquired two contiguous blocks of magnetic and time-domain electromagnetic (TDEM) data totaling 16,300 line-km at 200 m line spacing. The western Block1 (9,900 km) is flown in NS direction with nominal terrain clearance of 46 m for EM bird. The magnetic and TDEM data were designated as Geophysical Data Set 1079 (Report on Kabinakagami Lake airborne geophysical survey, 2015) and released to the public by MNDM. About 8,800 line-km of traverse data from Block 1 are used for DNN study.

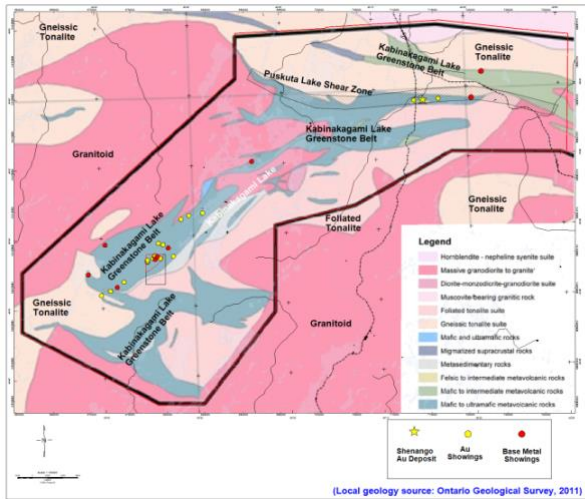


Figure 9. Local geology, base metal and gold mineralisation showings and the Shenango Au deposit of the selected VTEM survey area.

The descriptions of the KLGB geology are extracted from Wilson (1993) and are quoted below.

“The survey area is underlain largely by the Archean KLGB in the Wawa terrane of the Superior Province, Canadian Shield. As shown in Figure 9, the arcuate greenstone belt comprises primarily of mafic metavolcanic rocks. Metasedimentary rocks outcrop along the southeastern shore of Kabinakagami Lake, located in the west central region of the VTEM survey area. The greenstone belt had undergone low to intermediate amphibolite grade metamorphism. The plutonic rocks surrounding the greenstone belt are typically biotite or biotite-hornblende granodiorite to trondhjemite with gneissic tonalite. All units are cut by WNW-ESE and NE-SW trending diabase dykes.”

The RTP and EM induction time-constant TAU data of the Kabinakagami Lake TDEM survey area are presented in Figure 10. The locations of known gold mineralisation don't appear to coincide with the strongest conductors, but are located some distance away. Perhaps it is because the strongest conductors may be associated with pyrrhotite while gold mineralisation could be associated with pyrrhotite-pyrite mineral assemblage with pyrite dominating.

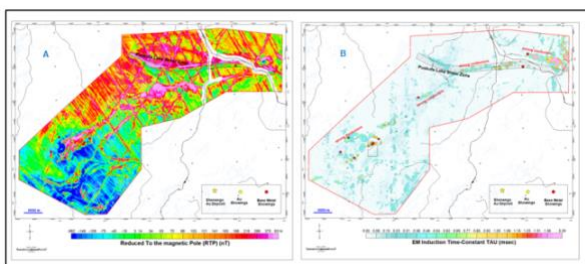


Figure 10. (A) Reduced-to-pole (RTP) data and (B) EM induction time-constant data of the Kabinakagami Lake TDEM survey area.

AIP mapping (Kwan et al., 2018) is applied to the EM data and the AIP apparent resistivity and the product $\log(aiip_res) * \text{Cole-Cole_time-constant}$ (Logrestau) data are presented in Figure 11.

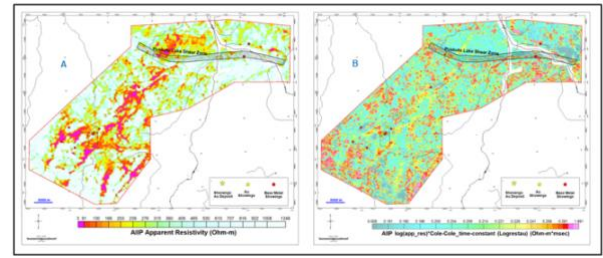


Figure 11. (A) AIP apparent resistivity and (B) AIP Logrestau.

All gold deposits and Au showings are located in the resistive zones. The Shenango Au deposit and two nearby showings are located in the strong Logrestau highs within the Puskuta Lake Shear Zone.

DNN Au predictive targeting is applied to the RTP, EM induction time-constant TAU, AIP apparent resistivity and Logrestau data. The DNN top 75% target probabilities are shown in Figure 12. The training and target areas are located in the SW region of the survey area with a group of known Au occurrences. The Au prospective DNN target zones cover all the known Au deposits and occurrences. In addition, there are high DNN probabilities in the SW region of the Kabinakagami Lake greenstone belt, which is worth looking into in future gold exploration.

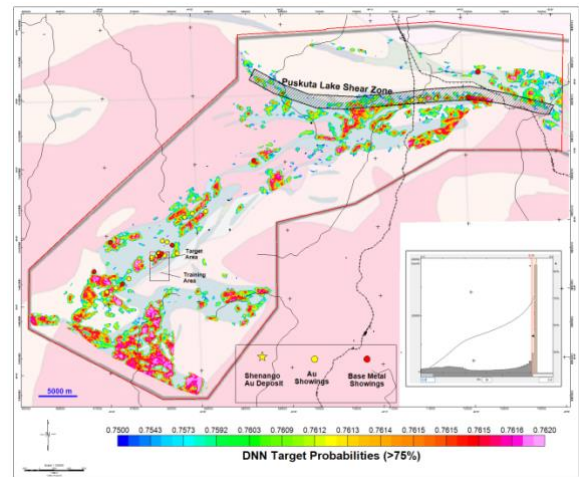


Figure 12. DNN top 75% predictive targeting probabilities for possible Au mineralisation in the of the Kabinakagami Lake TDEM survey area. The final DNN results are masked using the KLGB outline polygons.

CONCLUSIONS

The deep neural network predictive targeting method described here has been shown to be an effective tool in helping an interpreter of geophysical data to identify additional potential mineralisation. The supervised DNN approach requires a target area with either known mineral deposit/ occurrence, or in the absence of both a target area selected by an experienced interpreter. Through training, the DNN learns the geophysical signatures of the target area. The trained DNN is used to identify new targets with similar geophysical signatures.

We apply the DNN methods to a VMS case with strong magnetic/EM signatures and a gold case with weak

magnetic/EM signatures but some AIP responses. Results of both cases are worth further investigation.

The final selected DNN results must be treated with caution. They should be considered as just another information layer or constraint in target selection. The selection of final exploration targets must be carried out by an experienced interpreter using all available geoscientific data. One shouldn't apply DNN to geophysical data without distinct anomalous responses over the known deposits/occurrences. The inputs to a DNN must be carefully examined. Irrelevant data must be excluded. .

ACKNOWLEDGEMENTS

We thank Geotech for permission to publish the results of the study.

REFERENCES

- Goodfellow, I., Bengio, Y. and Courville, A., 2016: Deep Learning, MIT Press Book; <http://www.deeplearningbook.org>.
- Ontario Geological Survey, 2015, Ontario airborne geophysical surveys, magnetic and electromagnetic data, Kabinakagami Lake area: Ministry of Northern Development and Mines.
- Kwan, K., Legault, J.M., Johnson, I., Prikhodko, A. and Plastow, G., 2018, Interpretation of Cole-Cole parameters derived from helicopter TDEM data – Case studies: SEG, Expanded Abstracts, 5 pp.
- Kwan, K., Reford, S., Djiba, M., Pitcher, D.H., Bournas, N., Prikhodko, A., Plastow, G. and Legault, J.M., 2015, Supervised Neural Network Targeting and Classification Analysis of Airborne EM, Magnetic and Gamma-ray Spectrometry Data for Mineral Exploration: ASEG-PESA 24th International Geophysical Conference and Exhibition, Extended Abstracts, 4 pp.
- Legault, J.M., Izarra, C., Prikhodko, A., Zhao, S. and Saadawi, E.M., 2014, Helicopter EM (ZTEM-VTEM) survey results over the Nuqrah copper-lead-zinc-gold SEDEX massive sulphide deposit in the Western Arabian Shield, Kingdom of Saudi Arabia: Exploration Geophysics, 46 (1), 36-48.
- Mir, R., Perrouy, S., Thibaut A., Bérubé, C.L. and Smith, R.S., 2019, Structural complexity inferred from anisotropic resistivity: example from airborne EM and compilation of historical Resistivity/IP data from the gold-rich Canadian Malartic district, Québec, Canada, Geophysics (in press): 1-52, <https://doi.org/10.1190/geo2018-0444.1>.
- Reford, S., Lipton, G. and Ugalde H., 2004, Predictive ore deposit targeting using Neural Network analysis: SEG Expanded Abstracts, 1198-1201.
- Wilson, A.C. 1993, Geology of the Kabinakagami Lake greenstone belt: Ontario Geological Survey, Open File Report 5787, 80 pp.
- Witherly, K., R. Irvine, and E. B. Morrison, 2004, The Geotech VTEM time domain electromagnetic system: 74th Annual International Meeting, SEG, Expanded Abstracts, 1217–1221.